Multibody modelling of friction based interaction between turbine blades

Olivier Verlinden[1], Michal Hajžman[2], Hoai Nam Huynh[1], Miroslav Byrtus[2]

[1] Department of Theoretical Mechanics, Dynamics and Vibration
University of Mons
31, Bd Dolez, B-7000 Mons, Belgium
Olivier.Verlinden@umons.ac.be

[2] Faculty of Applied Sciences
University of West Bohemia
Univerzitni 22, 306 14 Plzen, Czech Republic
mhajzman@kme.zcu.cz

Abstract

Turbine blades are subjected to nozzle excitation frequencies that can correspond to eigen frequencies during acceleration and deceleration phases so that it is necessary to introduce some form of damping to avoid fatigue and mechanical damage of the blade material. Friction based solutions are nonlinear and offer the interesting property to operate only when the level of vibrations reaches some threshold. But they can be difficult to tune and the availability of a model proves helpful for the designer. The system analysed in this paper is an experimental device consisting of 2 blades, which interact with each other through a so-called friction element (FE), in contact with the shrouds placed at the tip of the blades. The system is expected to reproduce the vibration response of the blades subjected to axial forces. During past experimental campaigns, one of the blades was excited out-of-plane (axially with respect to the turbine) by an electromagnet and the displacements of the blade tips and friction element had been measured. Different models of the device have already been developed: comprehensive finite element model and in house models developed under `Matlab`. The latter possibly use different friction models, different kinematics of the friction element and can be based on time domain simulation or harmonic balance method.

In this paper, we present a multibody model developed within the framework EasyDyn. Due to the nonlinear effects of friction, the equations of motion are solved in the time domain. The contact is introduced by defining, for each surface, 4 points of the friction element interacting with a plane attached to the shroud. The purpose is to analyse the influence of some modelling options: rotation of the friction element, friction model, and normal force model and to draw rules concerning the possible simplifications. It turns out that the rotation of the friction element cannot be neglected if the normal contact stiffness is large. In this case, the deflection of the blades and the subsequent rotation of the blade shrouds make that the contact planes are no longer parallel, and that the bodies do not interact over the full expected contact surface. The contact stiffness will then have to be properly identified for reliable simulations.

1. Introduction

Turbine blades are subjected to severe vibration environments. Especially, nozzle excitation frequencies can correspond to eigen frequencies during acceleration and deceleration phases so that it is necessary to introduce some form of damping. Friction based solutions are nonlinear and offer the interesting property to operate only when the level of blade vibrations reaches some threshold. But they can be difficult to tune and the availability of a model proves helpful for the designer.

Friction in mechanical systems is an often investigated phenomenon [1], which can be found in many applications. Claeys et al. [2] introduced a complex bolted joint assembly intended to the investigation of friction effects on structural vibrations. They proved positive influence of friction and described some relations of excitation and energy dissipation. Blades and bladed disks are suitable systems where friction based solution can be employed [3]. Muszynska and Jones [4] modelled bladed disk as a simple lumped mass system and reported the effect of friction on the mistuning of the whole bladed disk.

Wu et al. [5] proposed an experimental device for the measurement of dry friction parameters for a chosen turbine blade material and utilized macroslip and microslip hysteresis models. Finite element modelling of blades and the harmonic balance method are used [6] in order to study the performance of tip pin dampers of different contact surfaces with respect to frequency response function. Friction bolt elements placed between blades are introduced and investigated in [7]. Real interaction of industrially used blades is treated numerically in [8], where the system is studied in frequency domain using rotational periodicity and the harmonic balance method.

The system which is analysed in this paper is the experimental prototype studied in [9], illustrated in Figure 1. It consists of 2 blades, which interact with each other through a so-called friction element (FE), in contact with the shrouds placed at the tip of the blades. During past experimental campaigns, one of the blades was excited out-of-plane by an electromagnet and the displacements of the blade tips and friction element had been measured. This type of arrangement was firstly the subject of a detailed finite element modelling in [10] including a comparison

with experiments in terms of eigen frequencies and modal dampings, evaluated from responses computed in the time domain, the system being nonlinear. Two types of friction models were compared: Coulomb's and a modified friction model where the friction coefficient decreases exponentially with the sliding velocity. A in-house model of the device has been specifically developed under `Matlab` in [11, 9]. The blades are modelled as flexible bodies comprising 5 Euler-Bernoulli beam elements while the shrouds and the friction element are modelled as rigid bodies. All motions are defined with respect to a rotating basis so that the centrifugal and Coriolis effects are possibly taken into account in the equations of motion. The normal component of the contact force between the surfaces is introduced through translational and rotational stiffnesses and dampings between the surfaces. The harmonic balance method was used in [11], Coulomb's friction being replaced by viscous damping so as to dissipate the same amount of energy. The poles of the system are analysed for different values of friction. In [9], the response of the system to a harmonic excitation is simulated in the time domain and compared to its experimental counterpart for different excitation levels. The modified friction model presented in [10] is retained. An interesting contribution is the development of a simplified model making the simulation much faster although less accurate. Two simplifications are proposed: on one hand, neglecting the rotation of the friction element and, on the other hand, assuming that the normal force is constant.

In this paper, we present a multibody model directly inspired from the one presented in [9, 11], developed within the framework EasyDyn [12]. Due to the nonlinear effects of friction, the equations of motion are solved in the time domain, as in [9]. The contact is introduced by defining, for each surface, 4 points of the friction element interacting with a plane attached to the shroud. The distance between the points is chosen so as to reproduce the torsional stiffness given in [9, 11]. The purpose is to analyse the influence of some modelling options: rotation of the friction element, friction model, and normal force model.

2. Description of the system and corresponding model

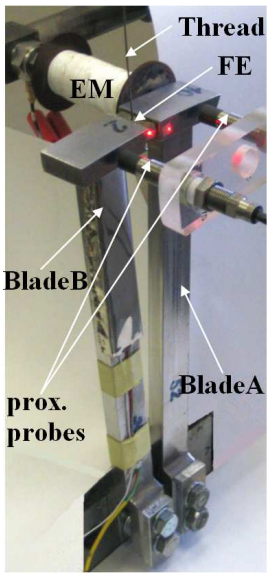

Figure 1: Experimental setup

The system under investigation (Figure 1) is composed of 2 blades clamped on a support replacing the turbine rotor. A friction element is placed between the blade ends. The blades are made of steel (Young modulus=2.1E11 N/m^2, Poisson coefficient 0.3, density 7800 kg/m^3) and have a rectangular cross section with a circumferential width of 20 mm and a transversal width of 10 mm. A Rayleigh damping is defined so as to get a damping ratio of 0.2 % for the first 2 flexural modes (α= 2.5133, β=1.41E-06). The blade ends and the friction element have a mass of 76 and 8.4 grammes respectively. Their inertia properties are computed assuming a parallelepipedic volume (Table 1). The geometry of the system is given in Figure 3.

Each blade is modelled by 4 beam elements, each of them involving 24 degrees of freedom. The motion of the friction element brings 6 more configuration parameters, leading to a total number of 54 degrees of freedom.

In order to prevent the friction element to get away from the contact area, it is maintained by a rope aligned with the direction of excitation. The latter is modelled by a spring whose stiffness k_f is equal to 10 N/m.

Table 1: Inertia characteristics of the rigid bodies

Body	*Mass (kg)*	I_{xx} *(radial, kg m^2)*	I_{yy} *(circumferential, kg m^2)*	I_{zz} *(axial, kg m^2)*
Blade end	0.0760	1.3991e-05	4.5917e-06	1.0666e-05
Friction element	0.0084	3.3695e-07	3.0520e-07	8.2152e-08

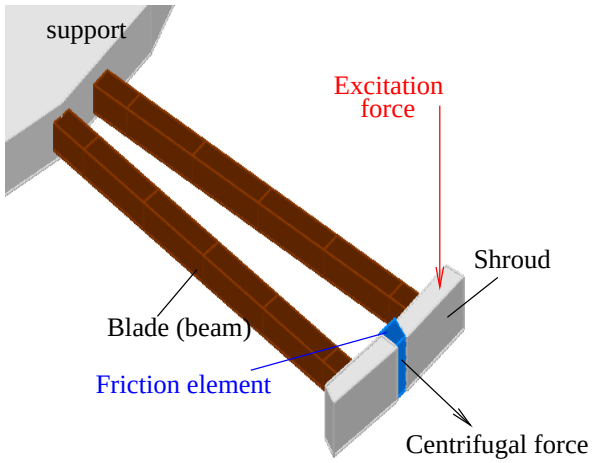

Figure 2: Global view of the model

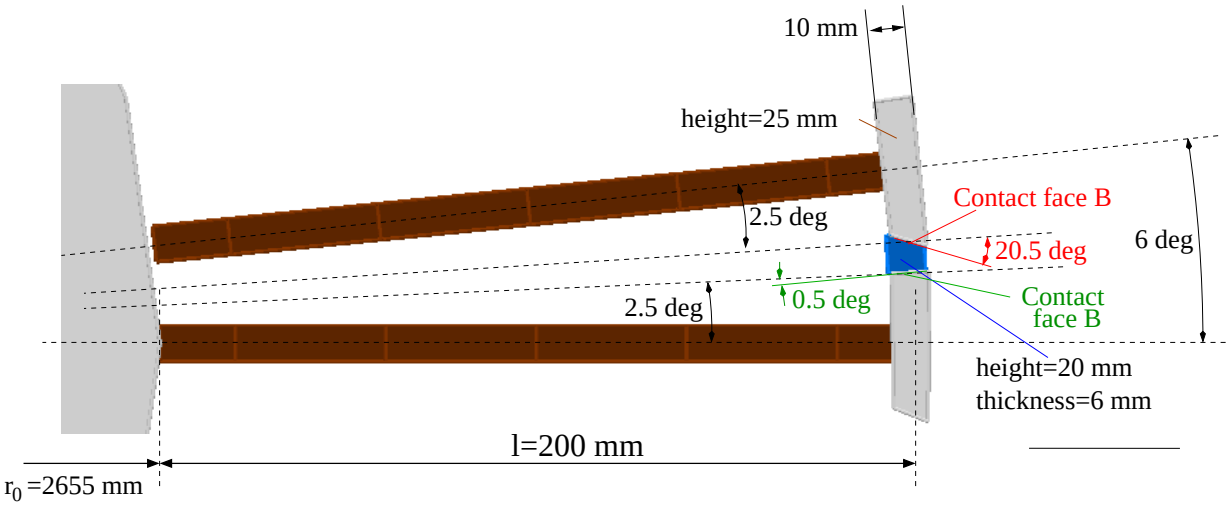

Figure 3: Geometry of the setup

The most important point of the model is the contact modelling. The planar contact between the friction and each blade end is modelled through 4 contact points placed at the vertices of a rectangle. The normal contact force F_n is calculated from the penetration δ of the contact point in the plane according to the well-known Hunt and Crossley law

$$F_n = K\delta^{p_K} + C\delta^{p_D}\dot{\delta} \text{ if } \delta > 0 \text{ and } F_n = 0 \text{ otherwise.} \quad (1)$$

The parameters have been adapted to align with the model presented in [11]: the p_K exponent is equal to 2 and the stiffness K_n of each contact point is equal to the fourth of the total stiffness K_{tot}, calculated in [11] from the material parameter σ and the contact area A as

$$K_{tot} = \frac{A}{\sigma^{p_K}}$$

Moreover, the radial and axial (Z) distances between the contact points have been chosen so as to get the same relation-

ship between the normal K_{tot} and the rotational K_θ stiffnesses. In [11], this relationship reads

$$K_\theta = K_{tot}\frac{b^2}{12} \tag{2}$$

where b is the contact area dimension perpendicularly to the axis corresponding to the rotational stiffness. In our model, the same rotational stiffness is obtained by defining a distance h between contact points, in the same direction as b

$$K_\theta = \frac{K_{tot}b^2}{12} = 2\left(K_n\frac{h^2}{2}\right) = \frac{K_{tot}}{2}\frac{h^2}{2} \rightarrow h = \frac{b}{\sqrt{3}} \tag{3}$$

Concerning the damping contribution, the exponent p_D is chosen as $(p_K-1)/2$ and the damping coefficient C is chosen so as to get a coefficient of damping of 20 % to stabilize the numerical integration. The corresponding data are detailed in Table 2.

Table 2: Parameters related to the normal contact force

Parameter	*Value*
Normal force exponent p_k	2
Height of contact faces	20 mm
Width of contact face A (B)	6 (6.39) mm
Stiffness coefficient on face A (face B) K	3.3333e12 (3.5473e12) N/m^2
Damping penetration exponent p_D	0.5
Damping coefficient on face A (face B)	4.73e4 (4.88e4) Ns/m$^{3/2}$

Table 3: Parameters related to friction

Parameter	*Value*
Static friction coefficient (GKF) μ_s	0.6
Dynamic friction coefficient (GKF or Coulomb) μ_d	0.3
Velocity threshold v^*	1e-3 m/s
Stribeck velocity V_{str}	0.5 m/s
Exponent γ	1
Contact tangential damping f_d	0

The tangential contact force depends on the normal force and on the sliding velocity. In the present model, the tangential contact force $\vec{\mathbf{F}}_t$ can be computed according to

- either a regularized Coulomb friction model

$$\vec{\mathbf{F}}_t = -\mu_d F_n \frac{\vec{\mathbf{v}}_s}{v^*} \tag{4}$$

- or a regularized GKF (General Kinetic Friction) model

$$\vec{\mathbf{F}}_t = -\left(\mu_d + (\mu_s-\mu_d)\exp(-(\|\vec{\mathbf{v}}_s\|/V_{str})^\gamma)\right)F_n\frac{\vec{\mathbf{v}}_s}{v^*} - f_d\vec{\mathbf{v}}_s \tag{5}$$

with $\vec{\mathbf{v}}_s$ the sliding velocity vector, μ_s and μ_d the static and dynamic friction coefficients respectively, V_{str} the Stribeck velocity, γ an exponent to adjust, f_d the damping coefficient and v^*=max$(\|\vec{\mathbf{v}}_s\|, V_{lim})$, V_{lim} being a threshold velocity to avoid numerical pitfalls for small sliding velocities. More physically, it is the velocity under which the sliding velocity is small enough to consider that the bodies stick to each other.

The friction parameters retained for this paper are listed in Table 3.

3. Reference simulation

The system is simulated during 10 s. To initiate the contact, the friction element is subjected to a radial force which increases linearly from 0 to 1 N during the first second. The corresponding total static normal force on faces A and B

are 2.75 N and 2.92 N respectively. The tangential force necessary to initiate slip of the friction element is then equal approximately to 1.7 N or 3.4 N for friction coefficients equal to 0.3 and 0.6 respectively.

From 2 to 8 seconds, one of the blades is subjected to a harmonic force perpendicular to the plane of the blades, i.e in the axial direction if referred to the turbine (Figure 2). The magnitude of this force is equal to 1 N, i.e. lower than the static force necessary to initiate the slip. In order to circumvent the difficulty to excite the system at the exact eigen frequency as in [9], the force is an exponential swept sine ranging from 125 to 145 Hz, so as to cross the first flexural eigen frequency of about 135 Hz. The Coulomb friction model is retained.

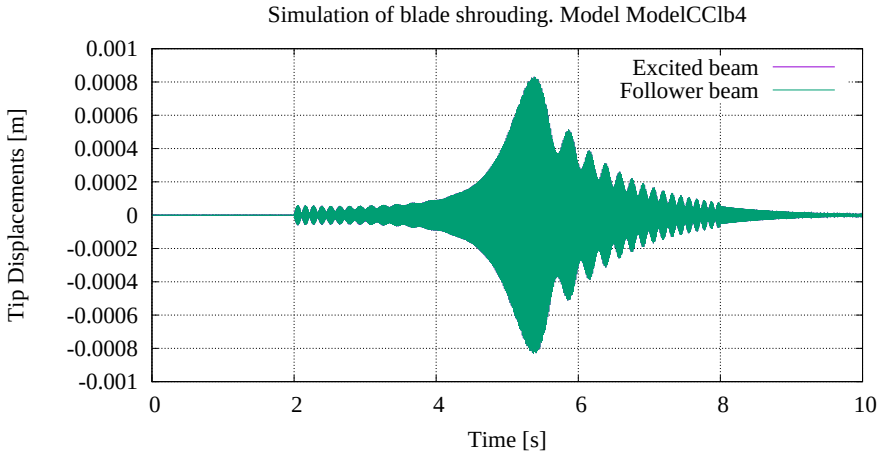

Figure 4: Reference simulation: displacement of blade ends

Figure 4 represents the displacement of the blade ends in the direction of excitation. As expected the amplitude of vibration increases up to the frequency of resonance and decreases afterwards. The displacements of the excited and follower beams (and consequently the friction element) are comparable, indicating that only microslips occur in the contacts.

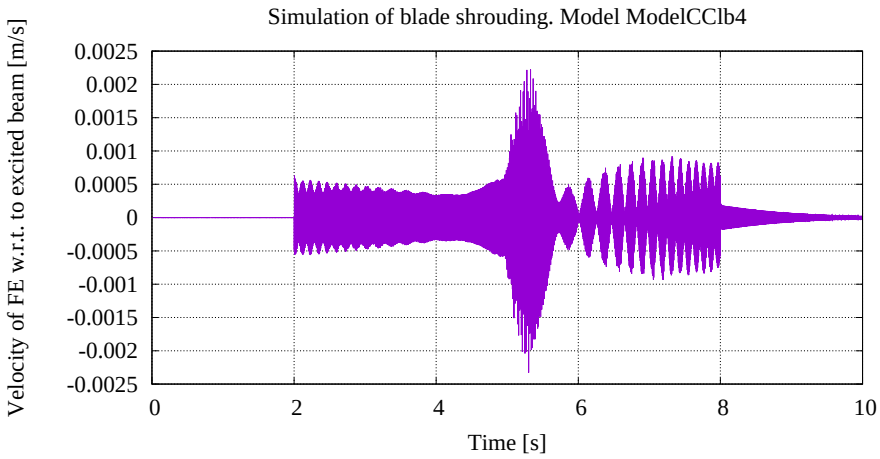

Figure 5: Reference simulation: relative velocity of friction element w.r.t. excited beam

This is confirmed by Figures 5 and 6 displaying the time histories of the relative velocities of the center of mass of the friction element with respect to the centers of the blade ends, projected along the direction of excitation. Indeed, the relative velocities remain most of the time under the chosen velocity threshold (0.001 m/s) so that it can be considered as stick. As we will see, this is not in agreement with the model presented in [9] where macroslips occur during resonance.

This can be explained by the evolution of the normal contact forces on both interfaces which is presented in Figures 7 and 8. At the beginning of the simulation, the normal force increases due to the progressive application of the radial

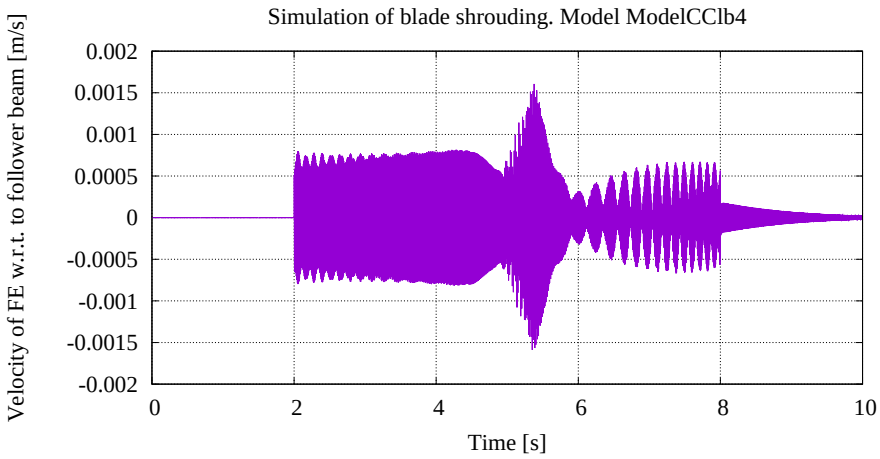

Figure 6: Reference simulation: relative velocity of friction element w.r.t. follower beam

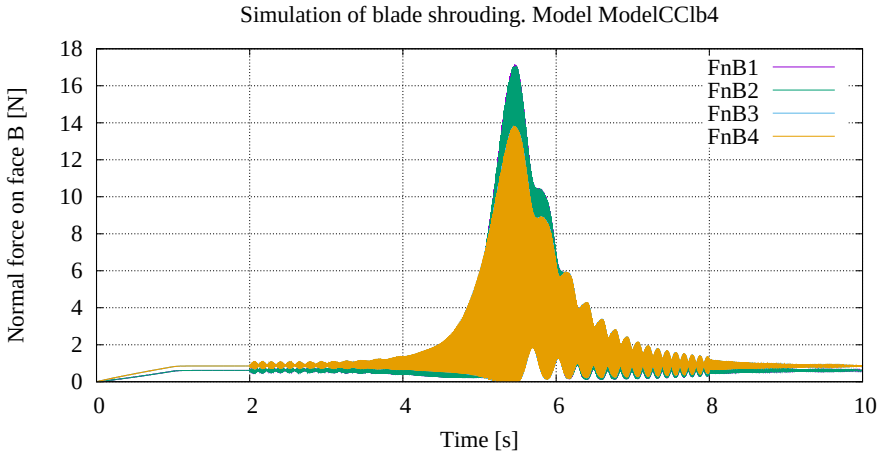

Figure 7: Reference simulation: normal contact forces at contact with excited beam

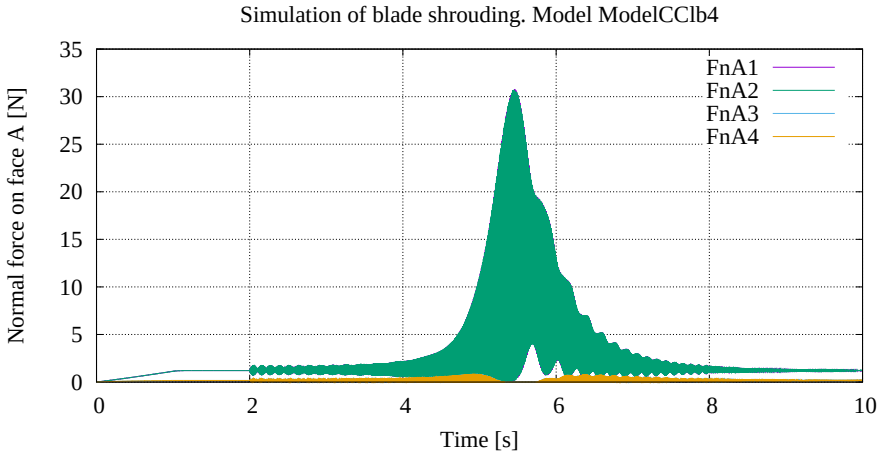

Figure 8: Reference simulation: normal contact forces at contact with follower beam

force on the friction element. Firstly, it appears that 2 points of face A are no longer in contact (Figure 8, points 3 and 4). This is explained by the bending of the blades which induce rotation of the blade shrouds, somehow "opening" the contact at the outer side. Secondly, the normal contact forces vary from the beginning of the application of the harmonic force and increase considerably during resonance. It is likely that the tangential forces applied on the friction element produce a radial moment which has to be balanced by normal forces. The phenomenon is similar to jamming: the tangential and normal components of the contact force increase together so that the friction limit is never reached.

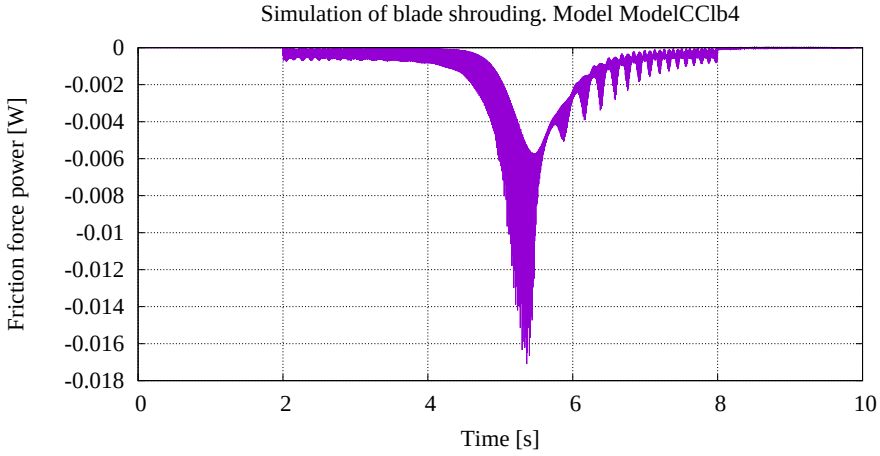

Figure 9: Reference simulation: power developed by friction forces

Finally, the power developed by the friction forces is plotted in Figure 9. It is of course negative and is larger about resonance. The integral of this power was integrated accurately during simulation and leads to a total loss of energy equal to 0.009 J which is, as we will see, rather low. The latter is particularly relevant in the context of the application and will be retained as a main indicator for comparing models.

4. Model simplification

Pesek et al proposed in [9] a simplified model neglecting on one hand the variation of the normal forces and on the other hand the rotation of the friction element. The effect of these hypotheses will be studied in this section.

The system was first simulated by locking the rotation of the friction element. This model will be referred to by model B. In that case, only one contact point is necessary with stiffness and damping parameters multiplied by 4.

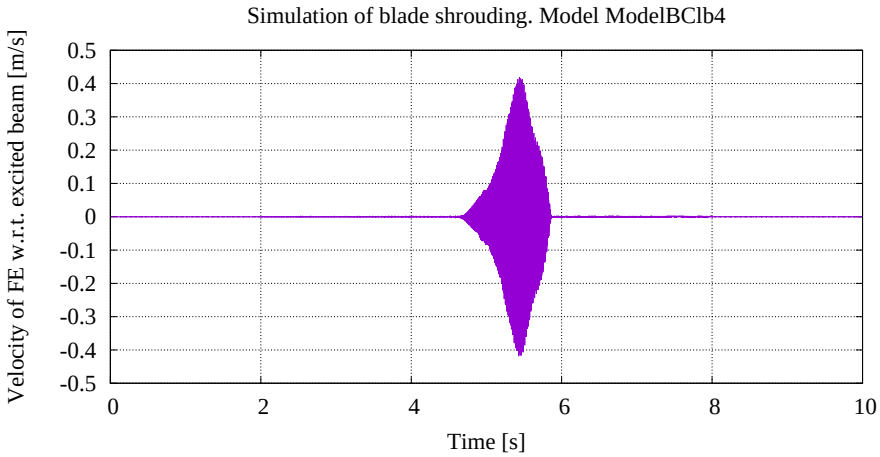

Figure 10: Model B: relative velocity of friction element w.r.t. excited beam

Figures 11 and 10 show the time histories of the relative velocities of the friction element with respect to the blades. It turns out that significant macroslips occur. Moreover, the observation of the normal contact forces (Figure 12) indicates

that they now remain quasi constant.

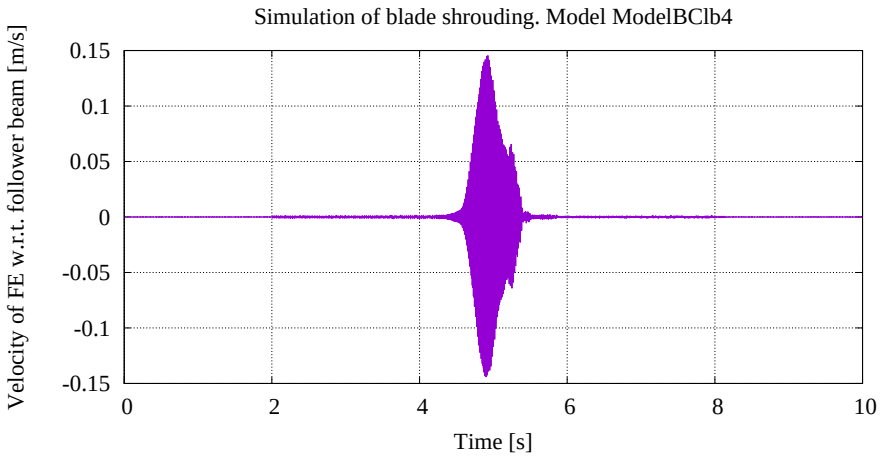

Figure 11: Model B: relative velocity of friction element w.r.t. follower beam

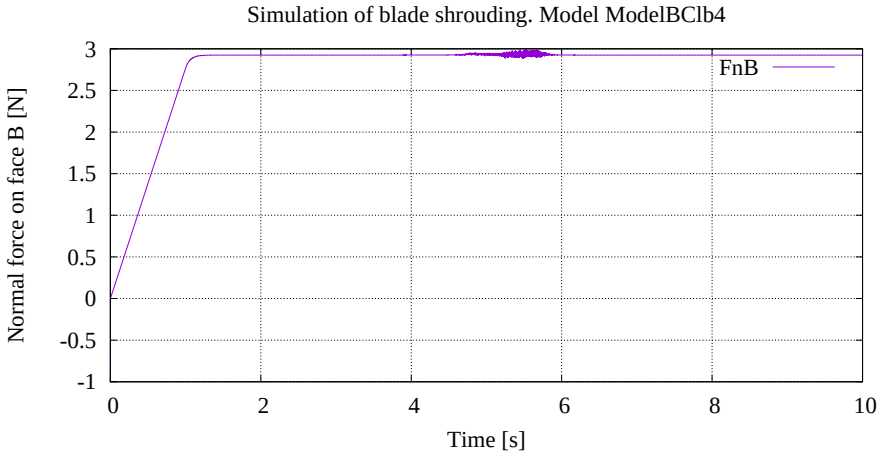

Figure 12: Model B: normal contact forces at contact with excited beam

Taking into account this last observation, one further simplification is made, consisting in keeping constant the normal force used for calulating the friction contribution, without degradation of the results (referred to by model A). The results in terms of dissipated energy are summarized in Table 4.

Table 4: Dissipated power for different models

	Full Model	*Model B*	*Model A*
Dissipated energy (J)	0.009	0.148	0.149

Models A and B actually compare positively with the simple `Matlab` model presented in [9]. As an example, the relative velocity of the friction element with respect to the excited beam, obtained with this model and model B, are compared in Figure 13. Although the rotation of the friction element is considered in the initial model, there is no update of the normal contact force due to moments along the radial axis, explaining the discrepancy with respect to model C.

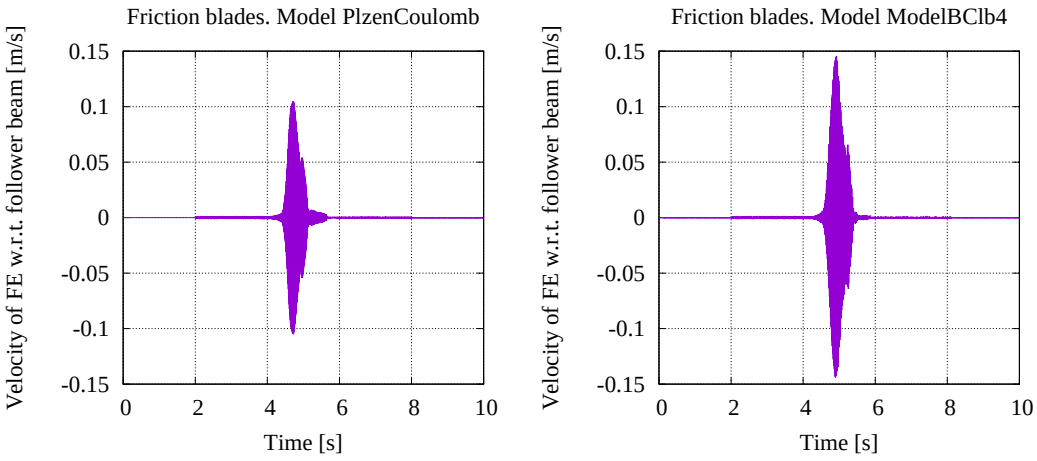

Figure 13: Comparison of relative velocity of friction element w.r.t. follower beam (left: initial, right: B)

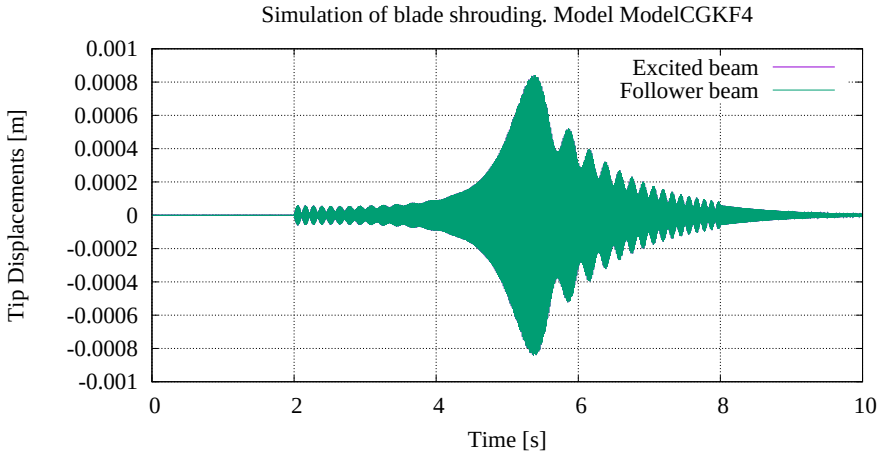

Figure 14: GKF friction model: displacement of blade ends

Figure 15: GKF friction model: relative velocity of friction element w.r.t. excited beam

5. Simulation with GKF model

Another option consists in using the GKF friction model in place of the Coulomb model. The results are illustrated in Figures 14 to 19.

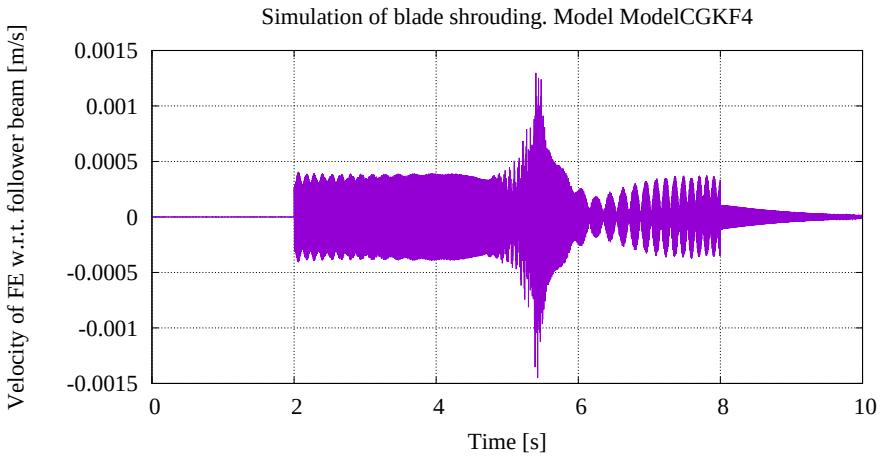

Figure 16: GKF friction model: relative velocity of friction element w.r.t. follower beam

As expected, the results do not depart from the ones obtained with the Coulomb's friction model. Indeed, the friction coefficient, evolving between 0.3 and 0.6, is always greater and also assures stick between the friction element and the blade shrouds. Practically the friction coefficient remains even close to 0.6 due to the low sliding velocities encountered in the contacts (Figures 15 and 16). The normal forces are comparable although a bit lower than with the Coulomb's friction model (Figures 18 and 17).

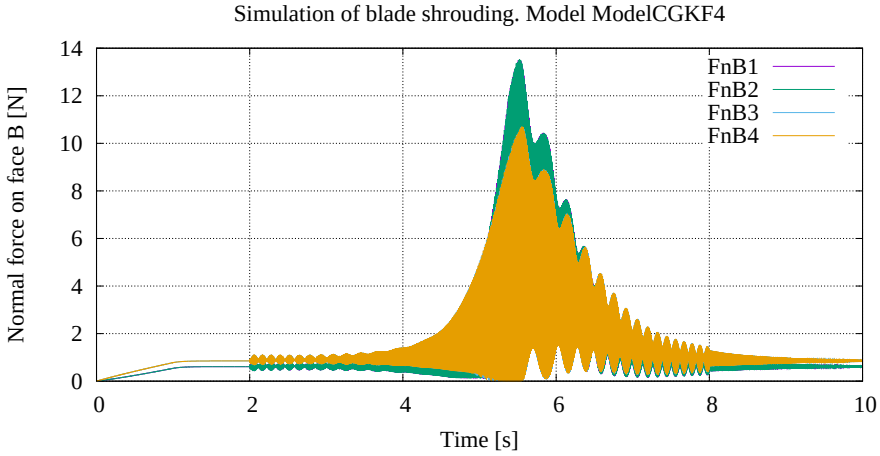

Figure 17: GKF friction model: normal contact forces at contact with excited beam

The time history of the power dissipated by friction is given in Figure 19. The total amount of dissipated energy is equal to 0.014 J and remains low.

6. GKF and simplified models

The simplifications presented previously (models A and B) have been tested with the friction GKF model. The same observations are made: the normal forces remain nearly constant (Figure 20) and significant macroslips occur around resonance (Figure 21). The dissipated energy is given in Table 5.

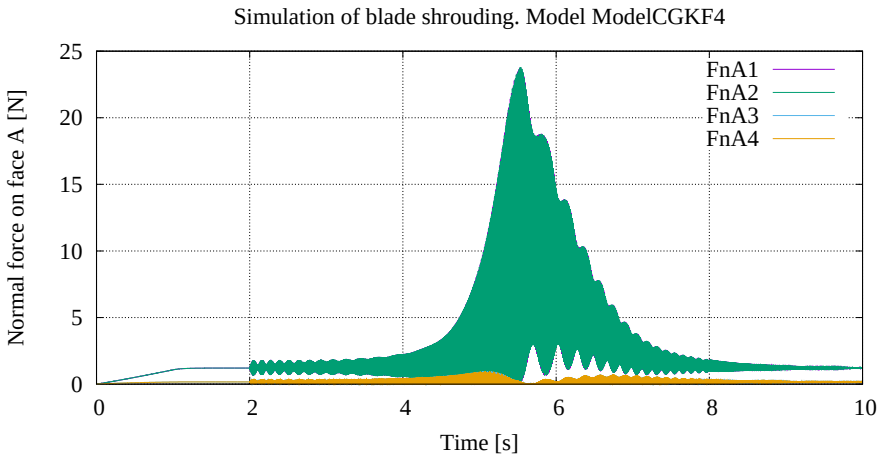

Figure 18: GKF friction model: normal contact forces at contact with follower beam

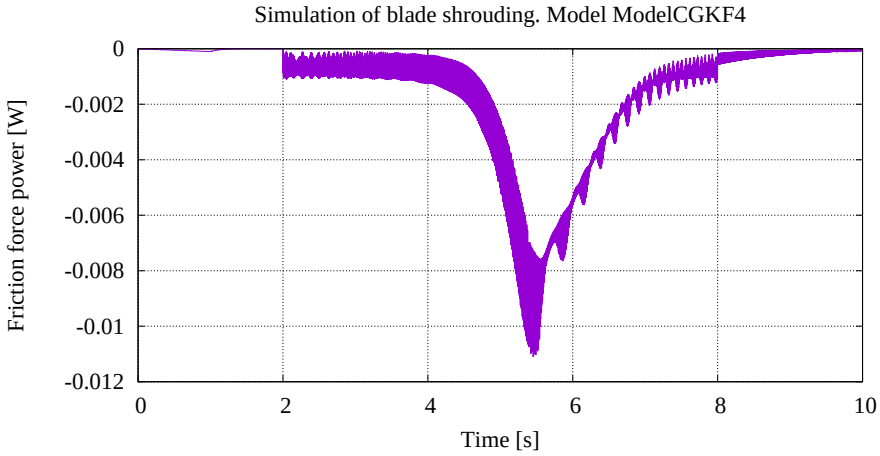

Figure 19: GKF friction model: power developed by friction forces

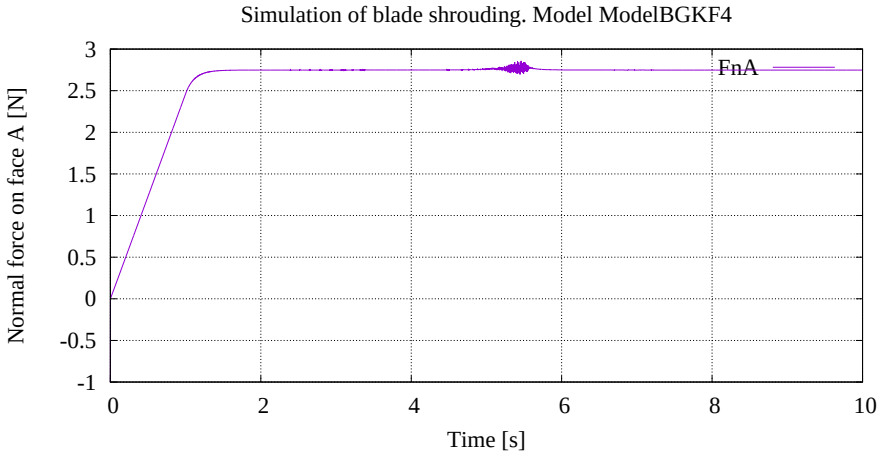

Figure 20: GKF friction model: normal contact force at contact with follower beam

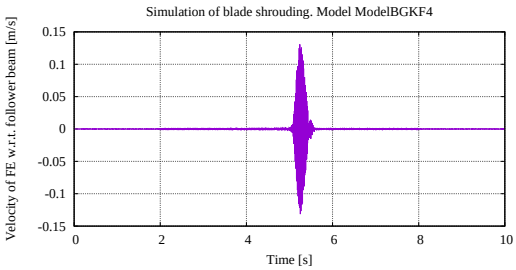

Figure 21: Relative velocity of friction element w.r.t. follower beam

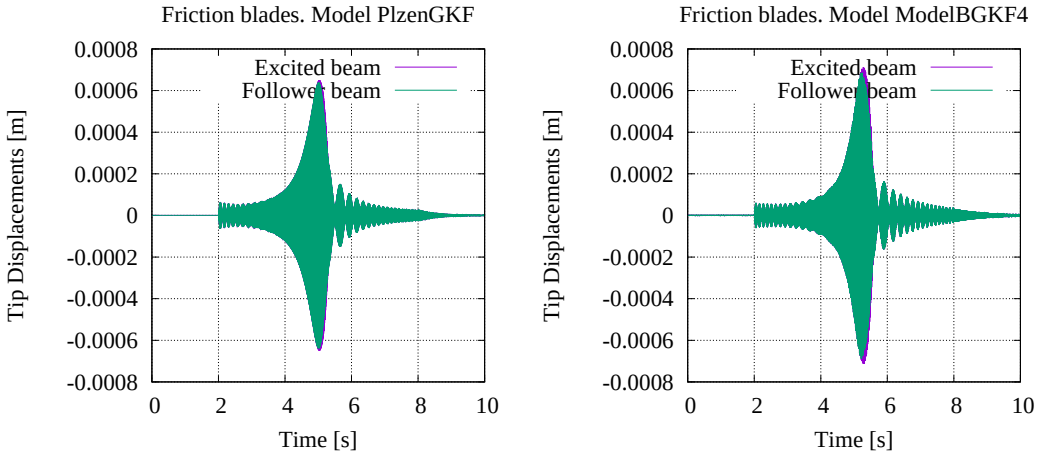

Figure 22: Comparison of relative velocity of friction element w.r.t. follower beam (left: initial, right: B)

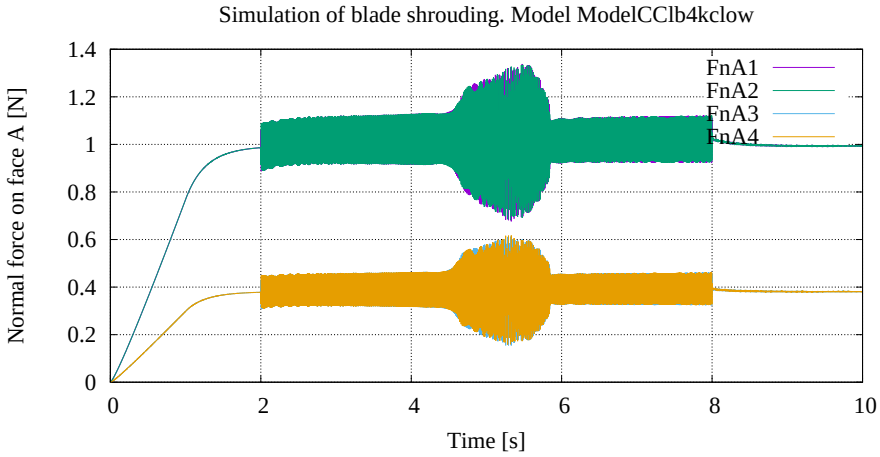

Figure 23: Soft contact and Coulomb: normal contact force at contact with follower beam

7. Simulations with different parameters

In order to understand the discrepancy between on one hand model C and, on the other hand, models A and B, some options have been changed: the stiffness k_f of the rope maintaining the friction element has been dropped, the contact damping was decreased to 5 % and the contact stiffness was considerably reduced ($\sigma = 3e-7$ in place of $\sigma = 3e-9$). Although the modifications of k_f and contact damping had no influence, the contact stiffness proved to be a key parameter whatever the friction model: with the more compliant contact stiffness, the normal contact forces become more stable (Figures 23 and 24) and models A, B, and C become consistent, as illustrated in Table 5 giving the total

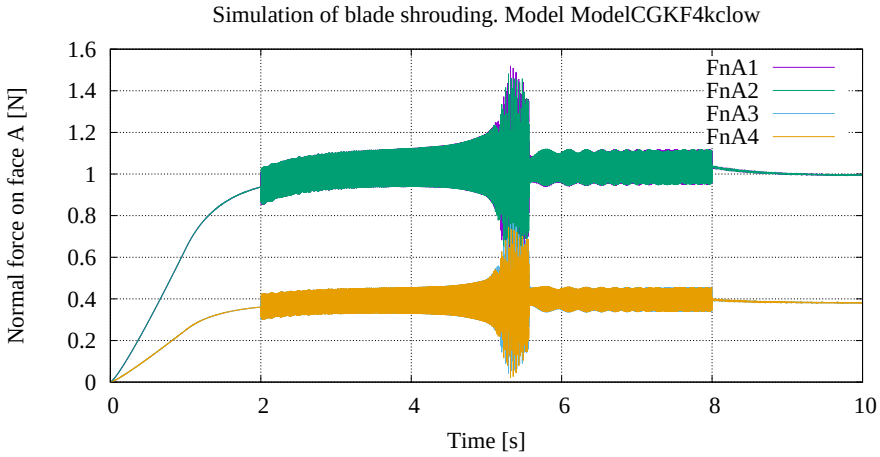

Figure 24: Soft contact and GKF: normal contact force at contact with follower beam

amount of dissipated energy for several models.

The simplified models A and B again show a good agreement with the model developed in [9], as illustrated in Figure 22.

Table 5: Dissipated power for various models

Coulomb	*Full Model with low contact stiffness*	*Model B*	*Model A*
Dissipated energy (J)	0.143	0.148	0.149
GKF	*Full Model with low contact stiffness*	*Model B*	*Model A*
Dissipated energy (J)	0.102	0.099	0.099

The impact of the decrease of the contact stiffness clearly appears in the evolution of the contact forces: the contact is now maintained at all points assuring a better balancing of moments. The question remains about the model which is the most representative of reality. It is of interest to remind that during the experimental measurements reported in [9], only microslips appeared in some cases although macroslips were showed by the model. The full model developed in ths paper is able to reproduce this phenomenon but several investigations still have to be performed to fully understand the physics of the phenomenon.

8. Conclusion

This paper was concerned with the simulation of the vibration response of two turbine blades interacting through a friction element by contact along a planar surface. The model is constructed according to the multibody approach, the blades correspond to flexible beams while the blade ends and the friction element are considered as rigid bodies. The contact is modelled as a force element. For each of the 4 contact points used to represent the surface contact, the normal force is calculated from the penetration and the penetration rate while the tangential force is calculated from the normal force and the sliding velocity according to the Coulomb's or GKF models endowed with regularization. The response of the system has been studied when subjected to out of plane force modulated by a logarithmic swept sine crossing the first bending resonance frequency. Different model options adopted in previous works have been analysed.

It turns out that it is possible to reproduce the results of the model developed in [9] after some simplifications, i.e. locking the rotation of the friction element (so that only one contact point can be used for each surface) and possibly keeping the same value of the normal force throughout simulation. However, the obtained results are not in agreement with the full model which demonstrates a large increase of the normal contact forces which lead somehow to the jamming of the contact. The analysis of the results shows that the stiffness of the contact, combined with the bending of the blades and consequently the rotation of the blade shrouds prevents the contact along the full surface. This partial loss of contact could be the explanation of the behaviour exhibited by the system. Using a reduced contact stiffness allowed to maintain a full contact and to get consistent results between full and simplified models. The practical conclusion is that the contact stiffness will have to be properly identified for reliable simulations.

Acknowledgments

The second author was supported by the project number TE01020068 in the framework of the "Competence Centres" programme of the Technology Agency of the Czech Republic.

The first and third authors would like to thank the Belgian National Fund for Scientific Research (FNRS-FRS) for the FRIA grant allotted to Hoai Nam Huynh.

References

[1] J. Awrejcewicz and P. Olejnik, "Analysis of Dynamic Systems With Various Friction Laws," *Applied Mechanics Reviews*, vol. 58, pp. 389-411, 2005.

[2] M. Claeys, J-J.Sinou, J-P.Lambelin and R.Todeschini, "Modal interactions due to friction in the nonlinear vibration response of the “Harmony” test structure: Experiments and simulations," *Journal of Sound and Vibration*, vol. 376, pp. 131–148, 2016.

[3] A. Rizvi, C. W. Smith, R. Rajasekaran and K. E. Evans, "Dynamics of dry friction damping in gas turbines: literature survey," *Journal of Vibration and Control*, vol. 22, no. 1, pp. 296-305, 2016.

[4] A. Muszynska and D. I. G. Jones, "On tuned bladed disk dynamics: some aspects of friction related mistuning," *Journal of Sound and Vibration*, vol. 86, no. l, pp. 107-128, 1983.

[5] J. Wu, R. Yuan, Z. He, D. Zhang and Y. Xie, "Experimental Study on Dry Friction Damping Characteristics of the Steam Turbine Blade Material with Nonconforming Contacts," *Advances in Materials Science and Engineering*, vol. 2015, Article ID 849253, dx.doi.org/101155/2015/849253.

[6] S. Zucca, T. Berruti and L. Cosi, "Experimental and numerical investigations on the dynamic response of turbine blades with tip pin dampers," *Journal of Physics: Conference Series*, vol. 744, 012131, 2016.

[7] R. Drozdowski, L. Völker, M. Höfele and D. M. Vogt, "Experimental and Numerical Investigation of The Nonlinear Vibrational Behavior of Steam Turbine Last Stage Blades with Friction Bolt Damping Elements," in *Proceedings of ASME Turbo Expo*, Montreal, GT2015-42244, 2015.

[8] J. Voldřich, J. Lazar and P. Polach, "Nonlinear Vibration Analysis of Steam Turbine Rotating Wheel Equipped with the LSB48 Blades," in *Proceedings of The 14th IFToMM World Congress*, Taipei, doi: 10.6567/IFToMM.14TH.WC.OS4.007, 2015.

[9] L. Pešek, M. Hajžman, L. Půst, V. Zeman, M. Byrtus and J. Brůha, "Experimental and numerical investigation of friction element dissipative effects in blade shrouding," *Nonlinear Dynamics*, vol. 79, pp 1711–1726, 2015.

[10] L. Pešek, L. Půst, F. Vaněk and J. Veselý, "FE modeling of Blade Couple with Friction Contacts under dynamic loading," in *Proceedings of the 13th World Congress in Mechanics and Machine Science*, Mexico, Paper IMD-123, 2011.

[11] M. Byrtus, M. Hajžman and V. Zeman, "Linearization of friction effects in vibration of two rotating blades," *Applied and Computational Mechanics*, vol. 7, pp. 5–22, 2013.

[12] O. Verlinden, L. Ben Fékih and G. Kouroussis, "Symbolic generation of the kinematics of multibody systems in EasyDyn: From MuPAD to Xcas/Giac," *Theoretical and Applied Mechanics Letters*, vol. 3, no. 1, paper 013012, http://dx.doi.org/10.1063/2.13013012, 2013.

[13] B. Armstrong-Hélouvry, P. Dupont and C. Canudas de Wit, "A survey of models, analysis tools and compensation methods for the control of machines with friction," *Automatica*, vol. 30, no. 7, pp 1083-1138, 1994.